Hindawi
Mathematical Problems in Engineering
Volume 2019, Article ID 9735368, 14 pages
https://doi.org/10.1155/2019/9735368

Research Article

Fuzzy Logic Optimization of Composite Brake Control Strategy for Load-Isolated Electric Bus

Yafei Xin,[1] Tiezhu Zhang,[1,2] Hongxin Zhang,[1,2] Qinghai Zhao,[1,2] Jian Zheng,[1] and Congcong Wang[1]

[1]*Mechanical and Electrical Engineering College, Qingdao University, Qingdao 266071, China*
[2]*Power Integration and Energy Storage Systems Engineering Technology Center, Qingdao University, Qingdao 266071, China*

Correspondence should be addressed to Hongxin Zhang; qduzhx@126.com and Qinghai Zhao; zqhbit@163.com

Received 10 June 2019; Revised 17 August 2019; Accepted 4 September 2019; Published 31 October 2019

Academic Editor: Roberta Di Pace

To improve the energy recovery rate and increase the driving range of load-isolated electric buses, a composite brake control strategy based on fuzzy logic optimization is proposed. Considering the influence of the battery SOC value and the braking intensity on the braking ratio, a fuzzy controller is designed for small and medium braking strengths to optimize the control strategy. The vehicle simulation model of the load-isolated electric bus was built with the AVL CRUISE software platform. The AVL CRUISE-Simulink cosimulation was carried out under the original control strategy and the optimized control strategy. The simulation results show that, under the premise of ensuring the stability of braking, the driving range of the vehicle with the optimized control strategy is increased by 7.74% and the energy recovery rate is increased by 11.05%.

1. Introduction

Regenerative braking, also known as braking energy recovery, is a new technology that is applied to new energy vehicles [1, 2]. Through the regenerative braking technology, part of the kinetic energy of an electric vehicle can be converted into electric energy. The electric energy is stored in the battery to improve energy utilization and increase the driving range [3, 4]. The load-isolated electric bus is an electric bus that isolates the engine from the load, ensuring that the engine is operating in the optimum efficiency zone. The regenerative braking system and the original hydraulic brake system of load-isolated electric buses constitute a composite braking system. Therefore, it is of research significance to study the composite braking energy recovery of electric buses.

Based on the fuzzy control theory, Li et al. [5] designed a regenerative braking control strategy for the power system of a fuel cell hybrid vehicle. The simulation verified the strategy to recover the braking energy and maintain the battery SOC (state of charge). To solve the hysteresis problem of hydraulic brake systems [6], a brake feel consistency control strategy was designed. A series control strategy was proposed for regenerative braking and pneumatic braking systems, and a road test was conducted [7]. A brake system with only motor/generator braking was proposed, and the effectiveness of the braking system was verified by simulations and experiments [8]. Using the fuzzy control method, Amirabadi and Farhangi [9] designed a control strategy for one-way and bidirectional converters in fuel cell hybrid vehicles. Considering the acceleration, jerk, and inclination of the vehicle, a regenerative braking fuzzy logic model was proposed [10]. For the regenerative braking system of fuel cell hybrid vehicles, Li et al. [11] proposed a fuzzy logic controller to improve the fuel economy of the vehicle. Considering the effects of the battery SOC, braking strength, and motor speed, Xiao et al. [12] proposed a regenerative braking strategy based on fuzzy control logic. Yuan et al. [13] proposed a new type of regenerative electrohydraulic composite braking system and proved its practicability through simulations and experiments.

The economics of the load-isolated electric bus are very good. If the regenerative braking technology is applied and the composite braking method is combined with the original mechanical brake, the energy-saving potential of the electric

bus will be largely realized [14, 15]. However, only a few studies have investigated the application of regenerative braking technology to load-isolated electric vehicles. This paper draws on the above research methods, combined with the actual situation of a load-isolated electric bus, and applies the regenerative braking method to the vehicles. This is a method improvement.

At the same time, the current research on control strategy optimization is mainly divided into two aspects: one is optimized by the Isight software and the other is optimized by the fuzzy toolbox of the MATLAB software. Using the MATLAB software optimization is to use the fuzzy toolbox and to set the fuzzy control rules for optimization. This paper uses MATLAB to optimize the control strategy and to propose a new fuzzy control rule and a fuzzy controller construction method.

Combined with the structure of the load-isolated electric bus, this paper proposes a series control strategy for the composite brake system. The fuzzy controller is designed for small braking and medium braking strengths to optimize the control strategy. Finally, the AVL CRUISE software and the Simulink software are used to carry out a cosimulation analysis on the proposed control strategy and optimization method to improve energy utilization and increase the driving range.

2. Load-Isolated Electric Bus Composite Brake Control Strategy

The experimental model in this paper is a load-isolated electric bus with rear-wheel drive. The load-isolated electric bus is a new type of electric car proposed by Qingdao University. It uses proprietary topology circuits and control strategies to protect the engine and energy storage batteries from changes in the vehicle load. At the same time, the engine is guaranteed to work in the best economic conditions, to improve the energy utilization rate of the vehicle and to increase the driving range. The load-isolated electric bus power source system consists of two roads: one is the energy storage battery-drive motor and the other is the engine-generator-power battery-drive battery. The energy storage battery is used as the main energy supply module to keep the bus run normally. When the energy storage battery SOC is reduced to the lowest power supply limit, the power battery system as an auxiliary energy module continues to provide energy to the bus. The design of the two batteries in the power system avoids the problem of overcharging and overdischarging of a single battery and ensures the running state of the electric bus.

A regenerative braking system is introduced in the brake system of the load-isolated electric bus, and a composite braking system is formed with the original mechanical friction braking system. The purpose of the regenerative braking system is to recover the braking energy as much as possible while improving the braking stability of the electric bus and to improve the energy utilization rate of the electric vehicle [16, 17]. The regenerative braking method only acts on the drive wheels, which in this paper, are the rear wheels of the electric bus.

2.1. Composite Brake System Structure. The brake system of the load-isolated electric bus includes a mechanical friction brake system and a motor regenerative brake system called the composite brake system. It is a brake energy recovery system. According to the coupling relationship between the feedback braking force and the friction braking force, the braking energy recovery system can be divided into a superimposed type (parallel type) and a coordinated type (series type).

The parallel brake energy recovery system superimposes the motor feedback braking force directly on the original friction braking force. It does not adjust the original friction braking force. The advantage is that the implementation is convenient, while the disadvantage is that the feedback efficiency is low and the braking feeling is poor. The principle of the series brake energy recovery system is to preferentially use the feedback braking force and then adjust the hydraulic braking force (or friction braking force) accordingly. It aligns the sum of the two braking forces with the total braking demand. The advantage is that the feedback efficiency is higher and the braking feeling is better. The disadvantage is that the traditional hydraulic brake system must be modified and the implementation is complicated. After comprehensive consideration, this paper uses a series braking energy recovery system, as shown in Figure 1, and carries out simulation modeling and analysis.

2.2. Braking Force Distribution Curve and Braking Force Distribution Method. In the composite brake system of the load-isolated electric bus, there are only a mechanical friction braking force on the front wheel and a mechanical friction braking force and a motor regenerative braking force on the rear wheel. The distribution relationship of each braking force is shown in Figure 2.

According to the ECE brake regulations proposed by the United Nations Economic Commission for Europe, this paper proposes a braking force distribution curve for the brake system of the load-isolated electric bus. As shown in Figure 3, the solid red line is the braking force distribution curve of the front and rear wheels of the load-isolated electric bus.

The dashed colored lines are r-line groups. The r-line group is a curve of the front and rear ground braking force when the front wheel is not locked and the rear wheel is locked.

The dashed green lines are the brake strength curves with different adhesion coefficients.

The purple line group is the f-line group. The f-line group is the relationship between the front and the rear ground braking force when the rear wheel is not locked and the front wheel is locked on various φ values.

The black line is the standard line of the ECE regulations.

The braking force distribution curve equation of the rear drive is

$$\frac{h_g}{GL}\left(F_{xb1}+F_{xb2}\right)^2+\frac{0.08\cdot h_g+b}{L}\left(F_{xb1}+F_{xb2}\right)-F_{xb1}+0.08\cdot\frac{Gb}{L}=0, \tag{1}$$

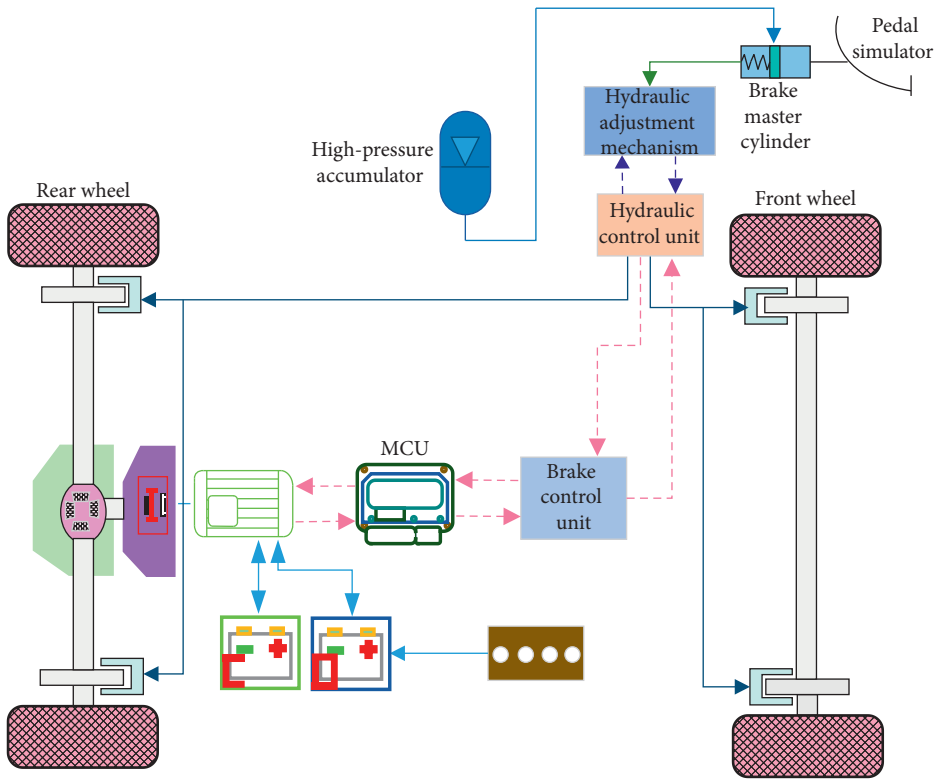

Figure 1: Composite brake system structure.

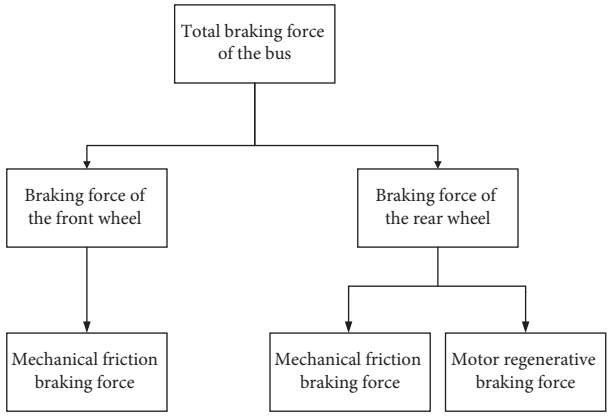

Figure 2: Distribution of the braking force of the composite brake system.

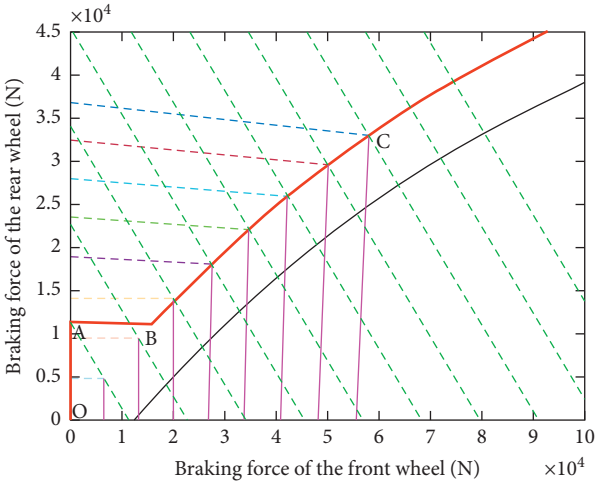

Figure 3: Braking force distribution curve.

where h_g is the vehicle's centroid height, G is the gravity of the vehicle, L is the wheelbase of the vehicle, F_{xb1} is the ground braking force of the front wheel, F_{xb2} is the ground braking force of the rear wheel, and b is the distance from the vehicle's center of mass to the rear axle.

The braking force distribution method of the front and rear wheels during the braking process of the load-isolated electric bus is as follows:

(1) When the braking strength of the electric bus $z \leq 0.1$, the braking strength is small. The braking force distribution curve of the small braking strength is shown in section OA in Figure 3. At this braking strength, the braking code does not restrict the braking force distribution of the front and rear wheels. To maximize the recovery of braking energy, only regenerative braking is used. Therefore, only the motor braking force of the rear wheel works, and the mechanical friction braking force of the front wheel and the rear wheel does not work.

The braking strength (z) is defined as follows, where du/dt is the deceleration of the vehicle and g is gravitational acceleration:

$$\frac{du}{dt} = zg. \tag{2}$$

At small braking strengths, the braking force distribution of the front and rear wheels of the electric bus is as follows:

$$\begin{cases} F_{bf} = 0, \\ F_{br} = mgz. \end{cases} \tag{3}$$

The specific distribution of the braking force between the front and the rear wheels is as follows:

$$\begin{cases} F_{bf-fric} = 0, \\ F_{br-fric} = 0, \\ F_{reg} = mgz. \end{cases} \tag{4}$$

In equations (3) and (4), F_{bf} is the braking force of the front wheels, F_{br} is the braking force of rear wheels, m is the quality of the vehicle, g is the acceleration of gravity, z is the braking strength, $F_{bf\text{-}fric}$ is the mechanical friction braking force provided by the front wheels, $F_{br\text{-}fric}$ is the mechanical friction braking force provided by the rear wheels, and F_{reg} is the regenerative braking force provided by the motor.

(2) When the braking strength of the electric bus $0.1 < z \le 0.234$, the braking strength is considered to be in the middle range. The braking force distribution curve of the middle braking strength is shown in section AB in Figure 3. In this braking strength, the braking force of the front and rear wheels of the electric bus is distributed according to the curve of $r = 0.234$. The r-line group is a curve of the front and rear ground braking force when the front wheel is not locked and the rear wheel is locked. At the middle braking strength, the braking force distribution of the front and rear wheels of the electric bus is as follows:

$$\begin{cases} F_{bf} = F_{req} - F_{br}, \\ F_{br} = \varphi\left(\dfrac{Ga}{L} - \dfrac{F_{req}h_g}{L}\right). \end{cases} \tag{5}$$

The specific distribution of the braking force between the front and the rear wheels is as follows:

$$\begin{cases} F_{bf-fric} = F_{req} - F_{reg}, \\ F_{br-fric} = 0, \\ F_{reg} = \varphi\left(\dfrac{Ga}{L} - \dfrac{F_{req}h_g}{L}\right), \end{cases} \tag{6}$$

where F_{req} is the total demand braking force of the vehicle, φ is the adhesion coefficient, and a is the distance from the vehicle's center of mass to the front axle.

(3) When the braking strength of the electric bus $0.234 < z \le 0.61$, the braking strength is large. The braking force distribution curve for the large braking strength is shown in section BC in Figure 3. At this braking strength, the braking force of the front and rear wheels of the electric bus is distributed according to an ideal braking force distribution curve (I curve).

At large braking strengths, the braking force distribution of the front and rear wheels of the electric bus is as follows:

$$\begin{cases} F_{bf} = \varphi F_{z1} = \varphi\dfrac{G}{L}\left(b + zh_g\right), \\ F_{br} = \varphi F_{z2} = \varphi\dfrac{G}{L}\left(a - zh_g\right). \end{cases} \tag{7}$$

The specific distribution of the braking force between the front and the rear wheels is as follows:

$$\begin{cases} F_{bf-fric} = 0, \\ F_{br-fric} = \max\left(0, F_{br-fric} - F_{reg}\right), \\ F_{reg} = \min\left(F_{br}, F_{reg-max}\right). \end{cases} \tag{8}$$

In equation (7), F_{z1} is the normal reaction force of the ground to the front wheel and F_{z2} is the normal reaction force of the ground to the rear wheel.

(4) When the braking strength of the electric bus $z > 0.61$, the braking strength is in the emergency range. To ensure the braking stability of the electric bus, regenerative braking is not used. The braking force requirement of the electric bus is satisfied by the mechanical friction braking force of the front and rear wheel brakes.

At the emergency braking strength, the braking force distribution of the front and rear wheels of the electric bus is as follows:

$$\begin{cases} F_{bf} = \varphi F_{z1} = \varphi\dfrac{G}{L}\left(b + zh_g\right), \\ F_{br} = \varphi F_{z2} = \varphi\dfrac{G}{L}\left(a - zh_g\right). \end{cases} \tag{9}$$

The specific distribution of the braking force between the front and the rear wheels is as follows:

$$\begin{cases} F_{bf-fric} = \varphi F_{z1} = \varphi\dfrac{G}{L}\left(b + zh_g\right), \\ F_{br-fric} = \varphi F_{z2} = \varphi\dfrac{G}{L}\left(a - zh_g\right), \\ F_{reg} = 0. \end{cases} \tag{10}$$

2.3. Compound Braking Control Strategy Logic. At present, the widely used braking force distribution control strategies are of series and parallel types. The series control strategy can be divided into the energy maximization control strategy, the sensory optimal control strategy, and the fuzzy logic control strategy. The parallel control strategy is divided into a simple parallel control strategy and an asynchronous parallel control strategy [18–20]. The advantages of the parallel control strategy are its simple structure, low cost, and good braking stability. Therefore, it is convenient to promote it in a wide range. The disadvantage is that the brake energy recovery rate is relatively low [21–23]. The energy recovery rate can be improved by optimizing the control strategies.

The serial control strategy is adopted in this paper. According to the proposed braking force distribution curve and the braking force distribution mode under each braking strength, the control strategy logic diagram of the compound braking system is shown in Figure 4. In the figure, Y represents YES and N represents NO in the control strategy proposed in this paper, except for the case in which the braking strength z takes into account "equal." The battery SOC signal (including the C_{soc} and the D_{soc}), the vehicle speed signal V, and the maximum regenerative braking force signal $F_{m\text{-}act}$ do not take into account "equal."

During the braking of the load-isolated electric bus, the sensor detects the brake pedal opening signal. After receiving the signal, the vehicle controller VCU determines the braking intention of the electric bus driver and the braking strength of the electric bus braking system. As shown in Figure 4, the magnitude of the braking force is determined by the control strategy logic.

When the braking strength $z \le 0.1$, the braking strength is small. For the purpose of protecting the battery, the energy storage battery SOC (C_{soc}) and the power battery SOC (D_{soc}) signals are comprehensively considered. Regenerative braking will not be used if both signals are greater than 80%. Mechanical brakes are used on the front and rear wheels. It is judged whether or not there is a signal of less than 80% among the two signals. If there is, then the velocity signal needs to be judged. It is not possible to use regenerative braking when the velocity signal V is lower than the minimum velocity V_{min}. V_{min} is the minimum velocity to perform regenerative braking. If at least one battery SOC set is less than 80% and the velocity signal V is also greater than the minimum velocity V_{min}, the actual maximum regenerative braking force $F_{m\text{-}act}$ of the motor is calculated by the control strategy. If $F_{m\text{-}act}$ is greater than the rear wheel demand braking force F_{br}, then the front wheel demand braking force is provided by the front wheel mechanical friction braking force, and the rear wheel demand braking force is provided by the motor regenerative braking force. The rear wheel mechanical friction braking force does not work. If $F_{m\text{-}act}$ is smaller than the rear wheel demand braking force F_{br}, then the front wheel demand braking force is provided by the front wheel mechanical friction braking force. The rear wheel demand braking force is provided by the rear wheel mechanical friction braking force and the motor regenerative braking force.

When the braking strength $0.1 < z \le 0.61$, the braking strength belongs to the middle and the large range. When $0.1 < z \le 0.234$, the braking strength belongs to the middle range. When $0.234 < z \le 0.61$, the braking strength is large. After receiving the SOC signal detected by the battery SOC sensor, the control strategy makes a logical determination. If both C_{soc} and D_{soc} are greater than 80%, all mechanical friction braking is used, and regenerative braking is not used. If at least one SOC signal is less than 80%, the control strategy further determines whether the vehicle speed signal V is less than V_{min}. If V is less than V_{min}, all mechanical friction braking is used.

If V is greater than V_{min}, the control strategy calculates the total demand braking force F_z and $F_{m\text{-}act}$. The front wheel demand braking force is provided by the front wheel mechanical friction braking force. The rear wheel demand braking force is determined by the size of $F_{m\text{-}act}$ and F_{br}. If $F_{m\text{-}act} > F_{br}$, the rear wheel demand braking force is provided by the motor regenerative braking force. If $F_{m\text{-}act} < F_{br}$, the rear wheel demand braking force is provided by the rear wheel mechanical friction braking force and the motor regenerative braking force.

When the braking strength $z > 0.61$, the braking strength is in the emergency range. To ensure the braking stability of the electric bus, regenerative braking is not used. The braking force is entirely provided by the mechanical friction braking force.

This paper models the control strategy of the composite brake system based on the proposed control logic.

3. Fuzzy Controller Design

In classical set theory, the membership of an element to a set can only take values of 0 and 1 to represent "belonging" and "not belonging." The fuzzy set theory shows that the membership degree can be any value in the interval [0, 1]. In the case of not accurately understanding the controlled object model, the fuzzy control theory optimizes the system through fuzzy rules. Because it does not need to know the exact mathematical model to get the output that meets a designer's vision, it has been widely used in the field of system control [24–27]. The fuzzy controller is the key technology in fuzzy control theory. It includes membership functions, fuzzy control rules, and influence surfaces. Designers make fuzzy rules according to the system environment and blur the input signal. Then, it is optimized by fuzzy rules. Finally, the output signal is obtained by defuzzifying [28–30].

In this paper, two different fuzzy controllers are designed for small and middle braking strengths. The small braking strength controller is a fuzzy controller with dual inputs and a single output. The middle braking strength controller is a three-input and dual-output fuzzy controller.

3.1. Fuzzy Controller for Optimizing Small Braking Strength Control Strategy

3.1.1. Input Variable and Output Variable. In a fuzzy controller with a small braking strength, there are two inputs

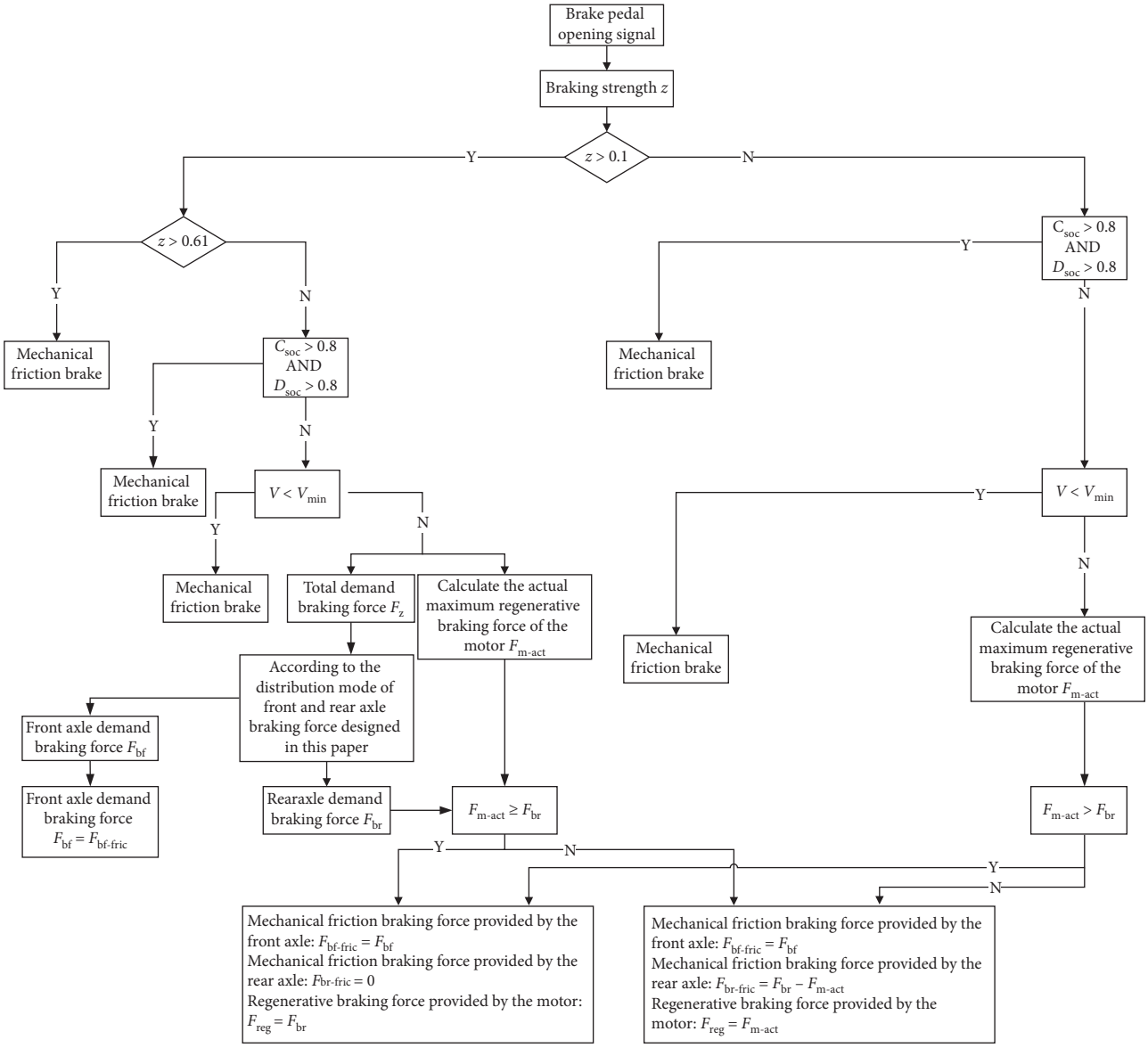

Figure 4: Complex brake control strategy logic diagram.

and one output. The two inputs are the energy storage battery SOC (C_{soc}) and the power battery SOC (D_{soc}). The one output is the regenerative braking ratio of the motor (REG), as shown in Figure 5.

3.1.2. Fuzzifying. The fuzzy subset of the input signal energy storage battery SOC (C_{soc}) is {L, M, H}, and the fuzzy domain is [0, 1]. The fuzzy subset of the power battery SOC (D_{soc}) is {L, M, H}, and the fuzzy domain is [0, 1]. According to the two input quantities and the one output quantity in the fuzzy controller, the corresponding membership functions are designed in the fuzzy toolbox in MATLAB. The input membership function is shown in Figure 6. Figures 6(a) and 6(b) show the membership functions of the input signals C_{soc} and D_{soc}, respectively.

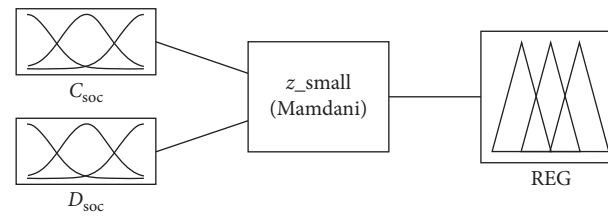

Figure 5: Fuzzy controller structure with small braking strength.

3.1.3. Fuzzy Control Rules. Fuzzy control rules are the core content of fuzzy controllers and are important factors affecting output signals. The fuzzy control rules established are shown in Table 1.

The fuzzy inference surface of the input and output is shown in Figure 7. The inference surface is observed by the

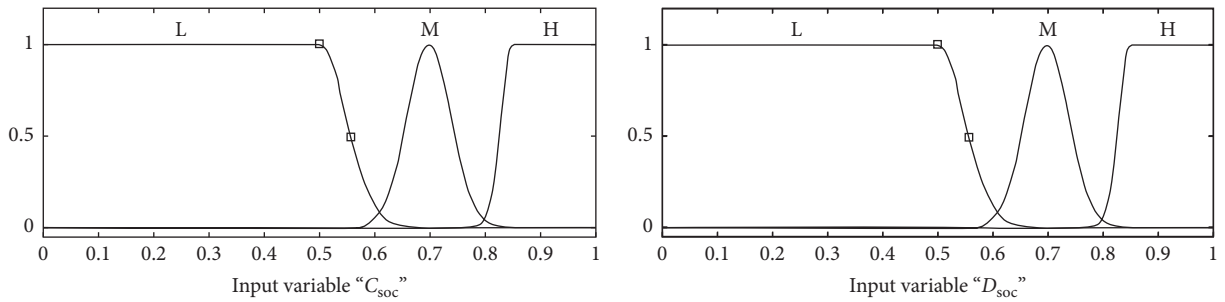

Figure 6: Input membership function of the small braking strength fuzzy controller.

Table 1: Fuzzy control rule table.

Regenerative braking ratio of the motor (REG)		Energy storage battery SOC (C_{soc})		
		L	M	H
Power battery SOC (D_{soc})	L	L	H	H
	M	H	H	M
	H	H	M	L

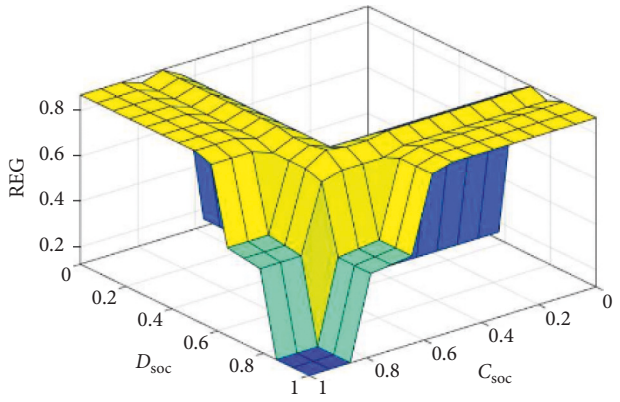

Figure 7: Regenerative braking ratio surface.

surface observer. It visually reflects the three-dimensional relationship between input and output.

Figure 7 describes the effect of C_{soc} and D_{soc} on the ratio of regenerative braking from the perspective of three-dimensional relationships.

3.1.4. Defuzzifying. The fuzzy subset of the output signal motor regenerative braking ratio REG is {L, M, H}, and the fuzzy domain is [0, 1]. Figure 8 shows a membership function of the output signal REG.

3.2. Fuzzy Controller for Optimizing Middle Braking Strength Control Strategy

3.2.1. Input Variable and Output Variable. In the middle braking strength fuzzy controller, there are three inputs and two outputs. The three inputs are the energy storage battery SOC (C_{soc}), the power battery SOC (D_{soc}), and the braking intensity (z). The two outputs are the motor regenerative braking ratio (REG) and the mechanical friction braking ratio (FRIC), as shown in Figure 9.

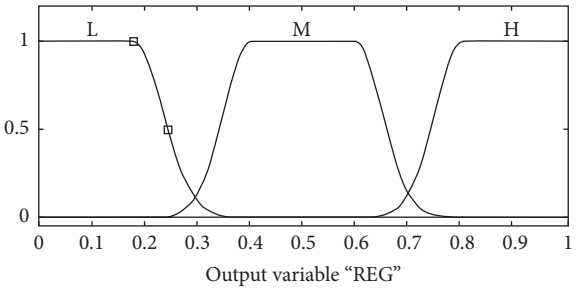

Figure 8: Output membership function of the small braking strength fuzzy controller.

3.2.2. Fuzzifying. The fuzzy subset of the input signal energy storage battery SOC (C_{soc}) is {L, M, H}, and the fuzzy domain is [0, 1]. The fuzzy subset of the power battery SOC (D_{soc}) is {L, M, H}, and the fuzzy domain is [0, 1]. The braking intensity z fuzzy subset is {L, M, H}, and the fuzzy domain is [0, 1]. The input membership functions are shown in Figure 10. Figures 10(a)–10(c) show the membership functions of the input signals C_{soc}, D_{soc}, and z, respectively.

3.2.3. Fuzzy Control Rules. The effects of C_{soc}, D_{soc}, and z on the motor regenerative braking ratio REG are shown in Table 2. The effects of C_{soc}, D_{soc}, and z on the mechanical friction braking ratio FRIC are shown in Table 3.

Figure 11(a) shows a fuzzy inference surface diagram of REG as a function of C_{soc} and D_{soc} for medium braking intensity. Figure 11(b) shows a curved surface diagram showing the influence of C_{soc} and z on REG in the middle braking strength. The effects of C_{soc} and z on REG are described from the perspective of three-dimensional relationships. The larger the C_{soc} and z, the smaller the motor regenerative braking ratio REG. This is also in line with the development of control strategies. It can be seen from Figure 11(b) that as the braking strength increases, the regenerative braking ratio of the motor gradually decreases, which is in accordance with the set rules of the control strategy.

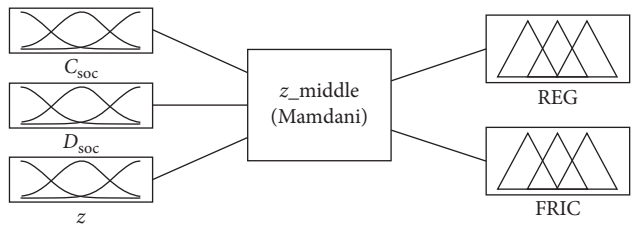

Figure 9: Middle braking strength fuzzy controller structure.

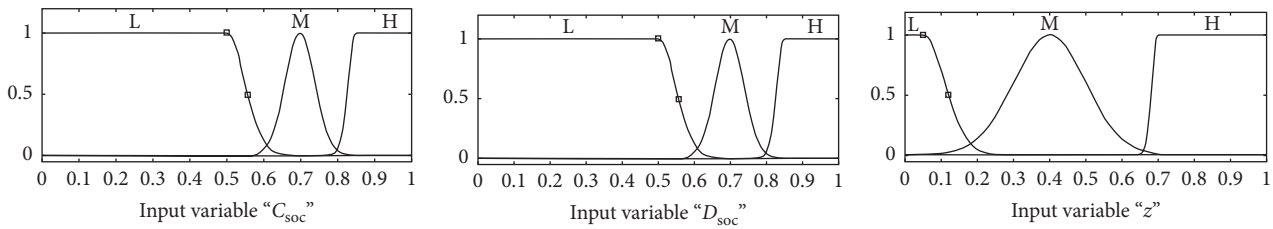

Figure 10: Input membership function of the middle braking strength fuzzy controller.

Table 2: Regenerative braking ratio control rules.

Judgement conditions	Results
(1) if (C_{soc} is L) and (D_{soc} is L) and (z is L)	then (REG is H)
(2) if (C_{soc} is L) and (D_{soc} is M) and (z is L)	then (REG is H)
(3) if (C_{soc} is L) and (D_{soc} is H) and (z is L)	then (REG is H)
(4) if (C_{soc} is L) and (D_{soc} is L) and (z is M)	then (REG is H)
(5) if (C_{soc} is L) and (D_{soc} is M) and (z is M)	then (REG is H)
(6) if (C_{soc} is L) and (D_{soc} is H) and (z is M)	then (REG is M)
(7) if (C_{soc} is L) and (D_{soc} is L) and (z is H)	then (REG is L)
...	...
(21) if (C_{soc} is H) and (D_{soc} is H) and (z is L)	then (REG is L)
(22) if (C_{soc} is H) and (D_{soc} is L) and (z is M)	then (REG is M)
(23) if (C_{soc} is H) and (D_{soc} is M) and (z is M)	then (REG is M)
(24) if (C_{soc} is H) and (D_{soc} is H) and (z is M)	then (REG is L)
(25) if (C_{soc} is H) and (D_{soc} is L) and (z is H)	then (REG is L)
(26) if (C_{soc} is H) and (D_{soc} is M) and (z is H)	then (REG is L)
(27) if (C_{soc} is H) and (D_{soc} is H) and (z is H)	then (REG is L)

Table 3: Friction braking ratio control rules.

Judgement conditions	Results
(1) if (C_{soc} is L) and (D_{soc} is L) and (z is L)	then (FRIC is L)
(2) if (C_{soc} is L) and (D_{soc} is M) and (z is L)	then (FRIC is L)
(3) if (C_{soc} is L) and (D_{soc} is H) and (z is L)	then (FRIC is L)
(4) if (C_{soc} is L) and (D_{soc} is L) and (z is M)	then (FRIC is L)
(5) if (C_{soc} is L) and (D_{soc} is M) and (z is M)	then (FRIC is M)
(6) if (C_{soc} is L) and (D_{soc} is H) and (z is M)	then (FRIC is M)
(7) if (C_{soc} is L) and (D_{soc} is L) and (z is H)	then (FRIC is H)
...	...
(21) if (C_{soc} is H) and (D_{soc} is H) and (z is L)	then (FRIC is H)
(22) if (C_{soc} is H) and (D_{soc} is L) and (z is M)	then (FRIC is M)
(23) if (C_{soc} is H) and (D_{soc} is M) and (z is M)	then (FRIC is M)
(24) if (C_{soc} is H) and (D_{soc} is H) and (z is M)	then (FRIC is H)
(25) if (C_{soc} is H) and (D_{soc} is L) and (z is H)	then (FRIC is H)
(26) if (C_{soc} is H) and (D_{soc} is M) and (z is H)	then (FRIC is H)
(27) if (C_{soc} is H) and (D_{soc} is H) and (z is H)	then (FRIC is H)

3.2.4. Defuzzifying. The fuzzy subset of the output signal motor regenerative braking ratio REG is {L, M, H}, and the fuzzy domain is [0, 1]. The fuzzy subset of the mechanical friction braking ratio FRIC is {L, M, H}, and the fuzzy domain is [0, 1]. The output membership functions shown in Figures 12(a) and 12(b) are the membership functions of the output signals REG and FRIC, respectively.

4. Control Strategy Fuzzy Logic Optimization Modeling

Based on the original control strategy, the fuzzy controller module in the MATLAB fuzzy toolbox is added. The fuzzy controller designed in Section 2 is added to the small and middle braking strength strategies to optimize the signal of the regenerative braking ratio and the friction braking ratio. Through the optimization of the fuzzy controller, the regenerative braking ratio and the energy utilization rate are increased [31, 32]. Figure 13 shows the model principle of the fuzzy controller. When the braking strength is small, the C_{soc} signal and the D_{soc} signal are input into the small braking strength fuzzy controller. After the calculation of the fuzzy rules and the fuzzy reasoning, the REG signal is outputted. When the braking strength is in the middle range, the C_{soc} signal, D_{soc} signal, and z signal are input into the middle braking strength fuzzy controller. Then, the output signals REG and FRIC are obtained by fuzzy reasoning.

The motor speed and torque characteristics are shown in Figure 14. When the battery is being charged, the relationship between the SOC and the voltage is shown in Figure 15.

5. Simulation Analysis of Optimal Control Strategy

5.1. Braking Stability Simulation Analysis. To verify the effectiveness of the optimal control strategy, the City_Cycle

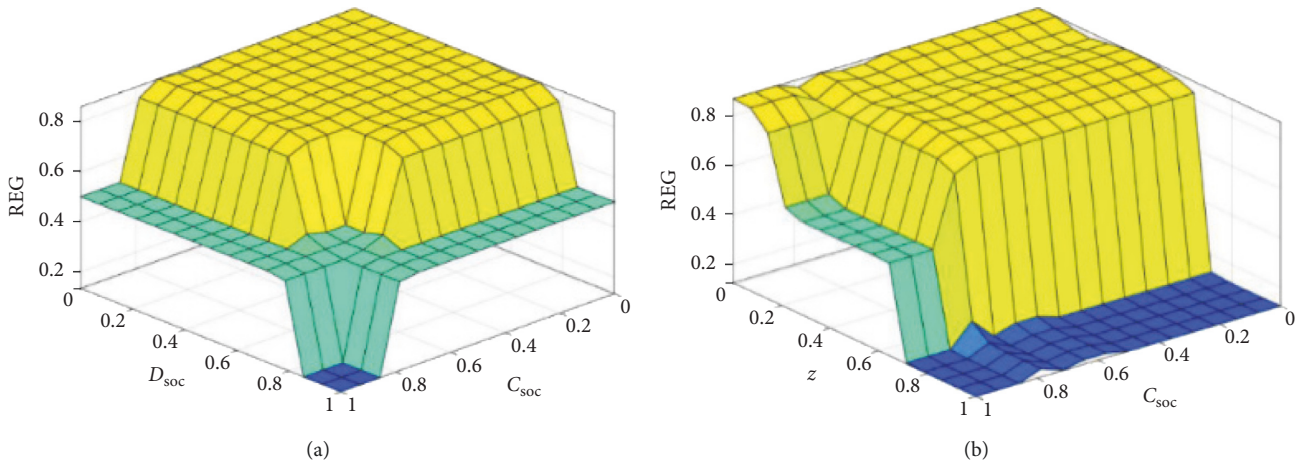

Figure 11: Regenerative braking ratio influence surface of the middle braking strength fuzzy controller.

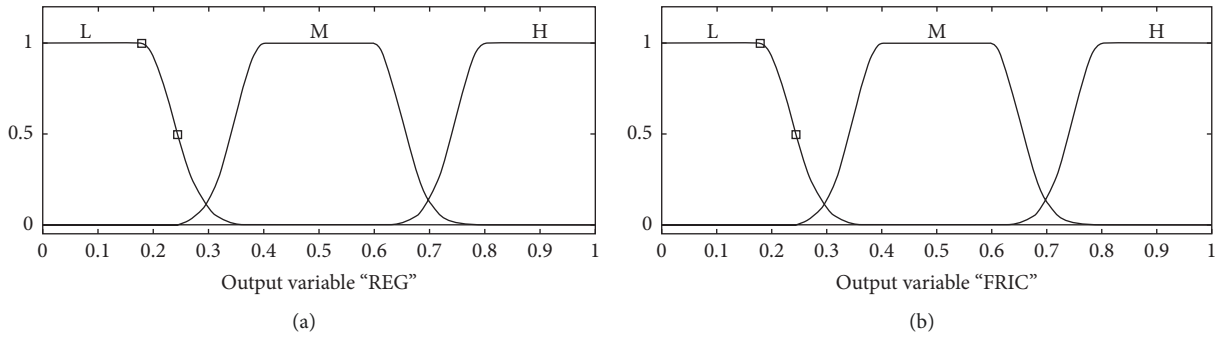

Figure 12: Output membership function of the middle braking strength fuzzy controller.

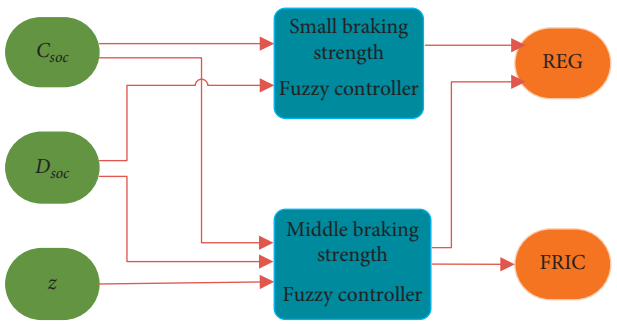

Figure 13: Fuzzy controller model.

cycle condition is selected for simulation analysis. The City_Cycle cycle condition is the typical urban bus cycle-driving condition in China. Table 4 shows the main parameters of the City_Cycle cycle.

Figure 16 shows the vehicle speed curve of a load-isolated electric bus.

It can be seen that the optimal control strategy satisfies the requirements of the working conditions very well, which indicates that the strategy has good working condition following characteristics. This is in line with the brake stability requirements.

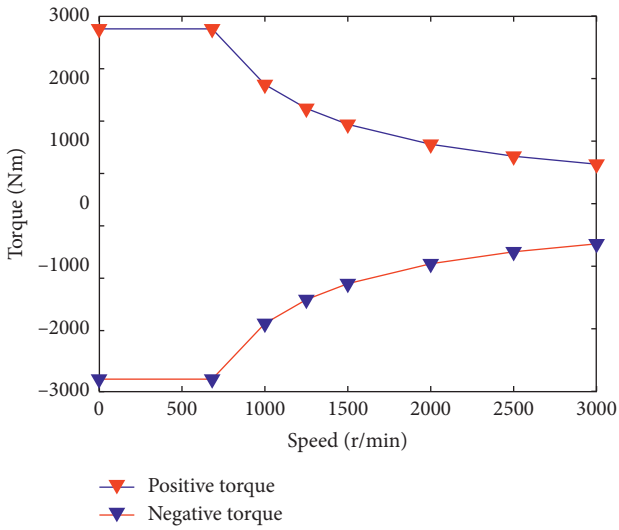

Figure 14: Motor characteristics.

5.2. Simulation Comparison between Original Strategy and Optimization Strategy under Single Working Conditions. In the single-mode simulation comparison, the initial SOC of the energy storage battery and the power battery is set to

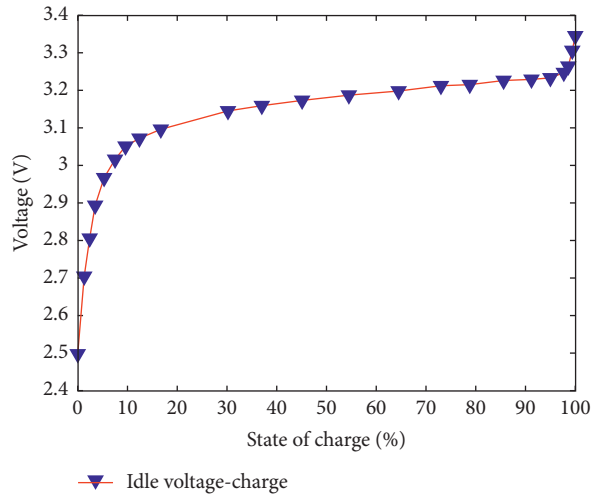

Figure 15: Battery characteristics.

Table 4: City_Cycle cycle condition.

Parameter	Value
Time (s)	1305
Maximum velocity (km·h^{-1})	60.38
Distance (km)	5.90
Maximum acceleration (m·s^{-2})	1.02
Maximum deceleration (m·s^{-2})	1.09
Parking times	14

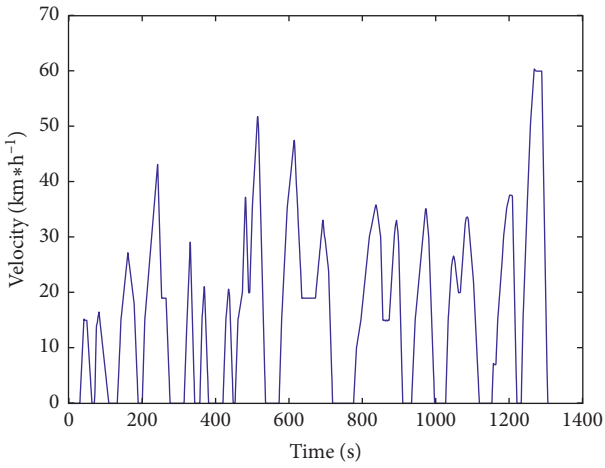

Figure 16: City_Cycle cycle driving condition.

50%. The vehicle runs a City_Cycle cycle condition. After the vehicle operating conditions are over, the motor torque, power battery input energy, power battery SOC, and energy recovery rate of the original control strategy and the optimized control strategy are compared. The energy flow during operation is shown in Figure 17.

5.2.1. Torque Comparison of the Drive Motor. The torque of the drive motor is shown in Figure 18. It can be seen from the figure that there is a greater increase in the torque of the optimal control strategy during braking. This shows that the control strategy is optimized to distribute more motor torque during braking.

5.2.2. Input Energy Comparison of Power Battery. The control strategy stipulates that the power battery is given priority to recover braking energy, as shown in Figure 19. The vehicle power battery embedded with the original control strategy recovered 7808.25 kJ of energy. The vehicle power battery embedded with the optimized control strategy recovered 11444.64 kJ of energy. The results show that the optimal control strategy can recover 3636.39 kJ more under the same road conditions.

5.2.3. SOC Comparison of Power Battery. Figure 20 shows a comparison of the power battery SOC. It can be seen from the diagram that the SOC of the vehicle power battery embedded with the optimal control strategy is 52.12% and the SOC of the vehicle power battery embedded with the original control strategy is 52.03%. The energy storage battery is the main power source, and the power battery is the auxiliary power source. Because the power battery preferentially recovers braking energy, the power battery SOC will rise. The results show that the power battery SOC of the optimized control strategy is 0.09% more than that of the original control strategy. This indicates that more regenerative braking ratios are allocated after optimization.

5.2.4. Energy Recovery Ratio Comparison. The energy recovery rates of the original control strategy and the optimized control strategy are shown in Table 5. The original control strategy was 35.79%, and the optimal control strategy was 52.88%. In terms of energy recovery, the optimal control strategy increased by 17.09%.

5.3. Simulation Analysis of Multicycle Conditions. The initial SOC of the energy storage battery and the power battery is set to 100%. Then, the load-isolated electric bus continues to operate in the City_Cycle condition until the set battery discharges the minimum SOC limit (C_{soc} is 20% and D_{soc} is 10%). After such testing, the energy recovery, economy, battery SOC, and charged energy of the control strategy can be detected.

5.3.1. Energy Recovery Rate Simulation Comparison. Under the original control strategy, the vehicle recovered 202121.47 kJ of energy, the energy consumption was 713712.24 kJ, and the energy recovery rate was 28.32%. Under the optimized control strategy, the vehicle recovered 141605.15 kJ of energy, the energy consumption was 359696.05 kJ, and the energy recovery rate was 39.37%, as shown in Table 6. The results show that the vehicle energy recovery rate of the embedded optimization control strategy increased by 11.05%.

5.3.2. Optimization Control Strategy Economic Simulation. The economic simulation results are shown in Table 7. The original control strategy has a driving range of 237.50 km

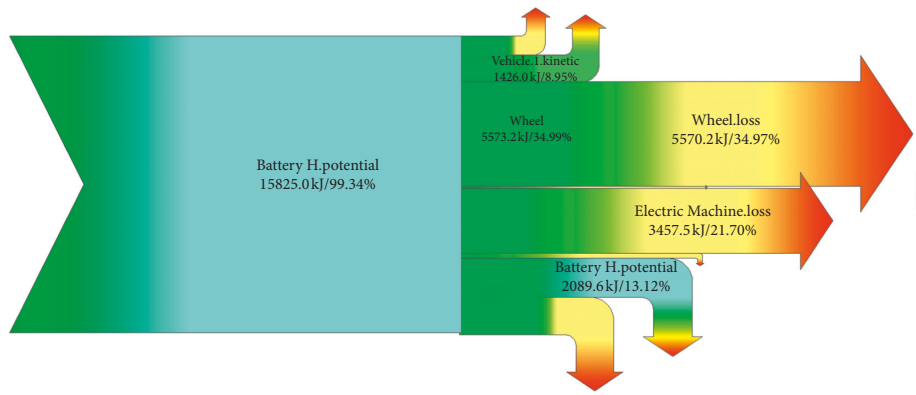

Figure 17: Energy flow.

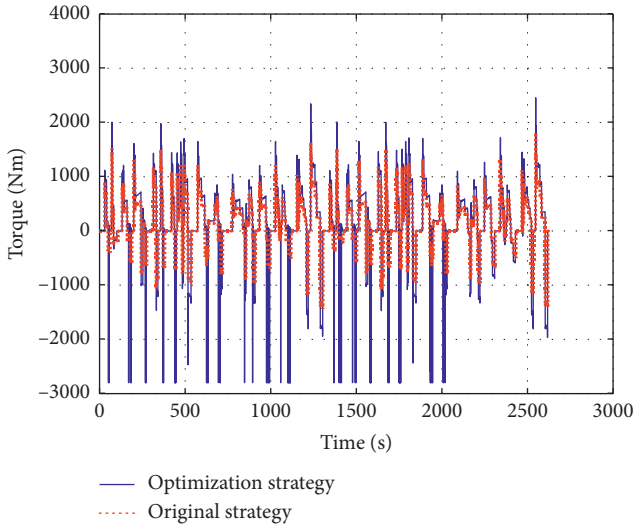

Figure 18: Drive motor torque comparison chart.

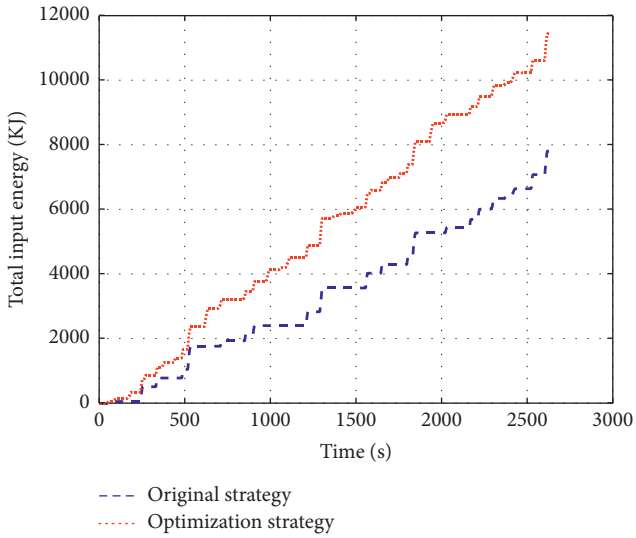

Figure 19: Power battery input energy comparison chart.

and a power consumption of 61.48 kWh per 100 kilometers. At the same time, the driving range of the optimized control strategy is 255.89 km, and the power consumption per 100 kilometers is 51.01 kWh. Compared with the original strategy, the driving range of the embedded optimization control strategy increased by 44 km, which is an increase of 7.74%. Moreover, the power consumption per 100 kilometers was reduced by 10.47 kWh, which is a reduction of 17.03%

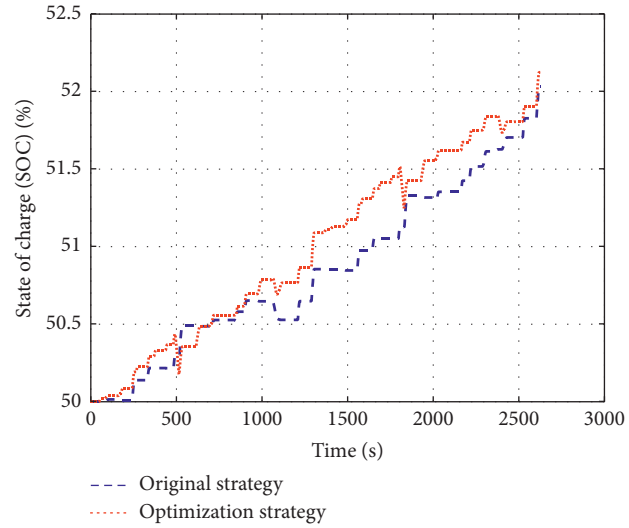

Figure 20: SOC comparison chart of the power battery.

5.3.3. Battery SOC Change of Optimized Control Strategy. It can be seen from Figure 21 that when the energy storage battery is discharged until the SOC is reduced to 10%, the power is supplied by the power battery. Figure 20 shows a graph of the battery SOC variation for an optimized control strategy. When the power battery is discharged until the SOC is reduced to 20%, it is no longer discharged. This result is in line with the expected control objectives.

5.3.4. Charging Energy of Optimized Control Strategy's Battery. The charging energy of the optimized control strategy's battery is shown in Figure 22. It can be seen from Figure 22 that both the energy storage battery and the power battery SOC are greater than 80% and that no energy is recovered. At 5000 s, the energy storage battery SOC is lower

Table 5: Comparison of energy recovery before and after optimization.

Driving cycle	Control strategy	Vehicle consumption energy (kJ)	Recycled braking energy (kJ)	Effective energy recovery (%)
City_Cycle	Original strategy	21816	7808.25	35.79
City_Cycle	Optimization strategy	21643	11444.64	52.88

Table 6: Comparison of energy recovery rates before and after optimization.

	Consumed energy (kJ)	Recovered energy (kJ)	Energy recovery rate (%)
Original control strategy	713712.24	202121.47	28.32
Optimization strategy	359696.05	141605.15	39.37

Table 7: Economic simulation results.

Control strategy	Driving range (km)	Electricity consumption per 100 kilometers (kWh)
Original control strategy	237.50	61.48
Optimization control strategy	255.89	51.01

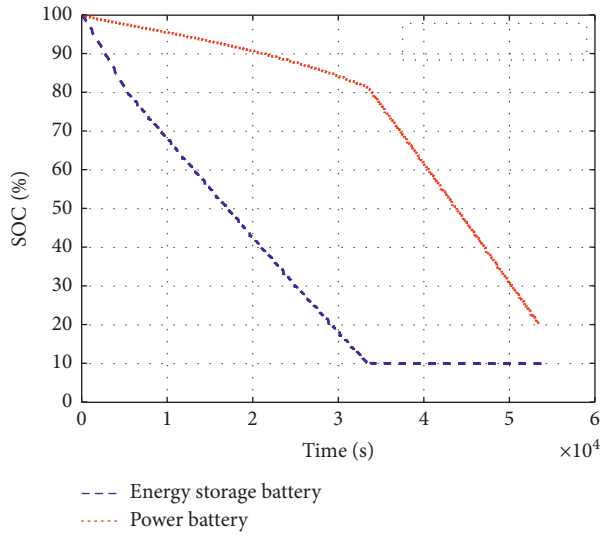

Figure 21: SOC change diagram of the optimization control strategy.

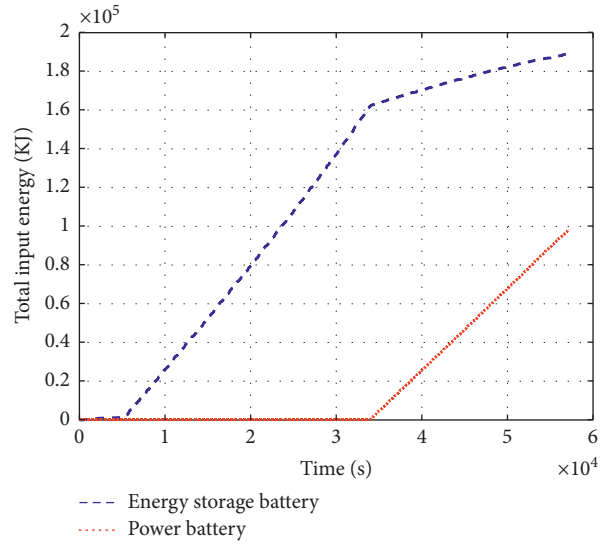

Figure 22: Charging energy graph of the optimization control strategy's battery.

than 80%, and energy recovery begins. At 35000 s, the power battery SOC is lower than 80%, and energy recovery begins.

6. Conclusions

In this paper, a regenerative braking system for the load-isolated electric bus was designed, and it provides a basis for research on the vehicle braking system. A series composite braking control strategy was proposed as the basis for further research on the composite braking of load-isolated electric buses.

This research designed two fuzzy controllers with small and medium braking strengths to optimize the series composite braking control strategy. The simulation analysis results show that the energy recovery rate of the optimized control strategy increased by 11.05% and the driving range increased by 7.74%. The effectiveness and rationality of the designed fuzzy controller are well verified. The results lay a foundation for the study of regenerative braking in the future.

Data Availability

The data used to support the findings of this study are included within the article.

Conflicts of Interest

The authors declare that there are no conflicts of interest regarding the publication of this paper.

Acknowledgments

This research work was supported by the National Key Research and Development Program of China (no. 2017YFB0102004), Shandong Province Major Innovation Engineering Project Subject (no. 2017CSGC0502), and

Shandong Province Key Research and Development Program (no. 2017GGX50106).

References

[1] G. Zhang, Z. Tian, P. Tricoli, S. Hillmansen, and Z. Liu, "A new hybrid simulation integrating transient-state and steady-state models for the analysis of reversible DC traction power systems," *International Journal of Electrical Power & Energy Systems*, vol. 109, pp. 9–19, 2019.

[2] W. Xu, H. Chen, H. Zhao, and B. Ren, "Torque optimization control for electric vehicles with four in-wheel motors equipped with regenerative braking system," *Mechatronics*, vol. 57, pp. 95–108, 2019.

[3] G. Xu, W. Li, K. Xu, and Z. Song, "An intelligent regenerative braking strategy for electric vehicles," *Energies*, vol. 4, no. 9, pp. 1461–1477, 2011.

[4] X. Cao and T. Ishikawa, "Optimum design of a regenerative braking system for electric vehicles based on fuzzy control strategy," *IEEJ Transactions on Electrical and Electronic Engineering*, vol. 11, pp. S186–S187, 2016.

[5] X. Li, L. Xu, J. Hua, J. Li, and M. Ouyang, "Regenerative braking control strategy for fuel cell hybrid vehicles using fuzzy logic," in *Proceedings of the 2008 International Conference on Electrical Machines and Systems*, pp. 2712–2716, Wuhan, China, October 2008.

[6] C. Wang, W. Zhao, and W. Li, "Braking sense consistency strategy of electro-hydraulic composite braking system," *Mechanical Systems and Signal Processing*, vol. 109, pp. 196–219, 2018.

[7] C. Qiu, G. Wang, M. Meng, and Y. Shen, "A novel control strategy of regenerative braking system for electric vehicles under safety critical driving situations," *Energy*, vol. 149, pp. 329–340, 2018.

[8] G. Xu, K. Xu, C. Zheng, X. Zhang, and T. Zahid, "Fully electrified regenerative braking control for deep energy recovery and maintaining safety of electric vehicles," *IEEE Transactions on Vehicular Technology*, vol. 65, no. 3, pp. 1186–1198, 2016.

[9] M. Amirabadi and S. Farhangi, "Fuzzy control of a hybrid power source for fuel cell electric vehicle using regenerative braking ultracapacitor," in *Proceedings of the 2006 12th International Power Electronics and Motion Control Conference*, pp. 1389–1394, Portoroz, Slovenia, August-September 2006.

[10] R. Maia, M. Silva, R. Araújo, and U. Nunes, "Electrical vehicle modeling: a fuzzy logic model for regenerative braking," *Expert Systems with Applications*, vol. 42, no. 22, pp. 8504–8519, 2015.

[11] X. Li, J. Li, L. Xu, and M. Ouyang, "Power management and economic estimation of fuel cell hybrid vehicle using fuzzy logic," in *Proceedings of the 2009 IEEE Vehicle Power and Propulsion Conference*, pp. 1749–1754, Dearborn, MI, USA, September 2009.

[12] B. Xiao, H. Lu, H. Wang, J. Ruan, and N. Zhang, "Enhanced regenerative braking strategies for electric vehicles: dynamic performance and potential analysis," *Energies*, vol. 10, no. 11, p. 1875, 2017.

[13] Y. Yuan, J. Zhang, Y. Li, and C. Li, "A novel regenerative electrohydraulic brake system: development and hardware-in-loop tests," *IEEE Transactions on Vehicular Technology*, vol. 67, no. 12, pp. 11440–11452, 2018.

[14] H. Zhang, G. Xu, W. Li, and M. Zhou, "Fuzzy logic control in regenerative braking system for electric vehicle," in *Proceedings of the 2012 IEEE International Conference on Information and Automation*, pp. 588–591, Shenyang, China, September 2012.

[15] G. Song and Y. Zhang, "Control strategy of energy recovery of electric vehicles based on braking strength," in *Proceedings of the 2016 35th Chinese Control Conference (CCC)*, pp. 8880–8884, Chengdu, China, July 2016.

[16] Y. Gao, L. Chen, and M. Ehsani, "Investigation of the effectiveness of regenerative braking for EV and HEV," in *Proceedings of the Future Transportation Technology Conference and Exposition*, Costa Mesa, CA, USA, August 1999.

[17] H. Gao, Y. Gao, and M. Ehsani, "A neural network based srm drive control strategy for regenerative braking in EV and HEV," in *Proceedings of the IEEE International Electric Machines and Drives Conference (Cat. No.01EX485)*, pp. 571–575, Cambridge, MA, USA, June 2001.

[18] N. J. Schouten, M. A. Salman, and N. A. Kheir, "Fuzzy logic control for parallel hybrid vehicles," *IEEE Transactions on Control Systems Technology*, vol. 10, no. 3, pp. 460–468, May 2002.

[19] X. Nian, F. Peng, and H. Zhang, "Regenerative braking system of electric vehicle driven by brushless DC motor," *IEEE Transactions on Industrial Electronics*, vol. 61, no. 10, pp. 5798–5808, 2014.

[20] R. Chicurel, "A compromise solution for energy recovery in vehicle braking," *Energy*, vol. 24, no. 12, pp. 1029–1034, 1999.

[21] J. Zhang, Y. Li, C. Lv, and Y. Yuan, "New regenerative braking control strategy for rear-driven electrified minivans," *Energy Conversion and Management*, vol. 82, pp. 135–145, 2014.

[22] J. Zhang, C. Lv, M. Qiu, Y. Li, and D. Sun, "Braking energy regeneration control of a fuel cell hybrid electric bus," *Energy Conversion and Management*, vol. 76, pp. 1117–1124, 2013.

[23] Z. Zhang, G. Xu, W. Li, and L. Zheng, "Regenerative braking for electric vehicle based on fuzzy logic control strategy," in *Proceedings of the 2010 2nd International Conference on Mechanical and Electronics Engineering*, Kyoto, Japan, August 2010.

[24] J. Ruan, P. D. Walker, P. A. Watterson, and N. Zhang, "The dynamic performance and economic benefit of a blended braking system in a multi-speed battery electric vehicle," *Applied Energy*, vol. 183, pp. 1240–1258, 2016.

[25] F. Naseri, E. Farjah, and T. Ghanbari, "An efficient regenerative braking system based on battery/supercapacitor for electric, hybrid, and plug-in hybrid electric vehicles with BLDC motor," *IEEE Transactions on Vehicular Technology*, vol. 66, no. 5, pp. 3724–3738, 2017.

[26] J. Ko, S. Ko, H. Son, B. Yoo, J. Cheon, and H. Kim, "Development of brake system and regenerative braking cooperative control algorithm for automatic-transmission-based hybrid electric vehicles," *IEEE Transactions on Vehicular Technology*, vol. 64, no. 2, pp. 431–440, 2015.

[27] W. Enang and C. Bannister, "Modelling and control of hybrid electric vehicles (a comprehensive review)," *Renewable and Sustainable Energy Reviews*, vol. 74, pp. 1210–1239, 2017.

[28] D. Paul, E. Velenis, D. Cao, and T. Dobo, "Optimal $\mu $ -Estimation-Based regenerative braking strategy for an AWD HEV," *IEEE Transactions on Transportation Electrification*, vol. 3, no. 1, pp. 249–258, 2017.

[29] D. Gao, Z. Jin, and Q. Lu, "Energy management strategy based on fuzzy logic for a fuel cell hybrid bus," *Journal of Power Sources*, vol. 185, no. 1, pp. 311–317, 2008.

[30] G. Yin and X. Jin, "Cooperative control of regenerative braking and antilock braking for a hybrid electric vehicle," *Mathematical Problems in Engineering*, vol. 2013, Article ID 890427, 9 pages, 2013.

[31] S. Heydari, P. Fajri, M. Rasheduzzaman, and R. Sabzehgar, "Maximizing regenerative braking energy recovery of electric vehicles through dynamic low-speed cutoff point detection," *IEEE Transactions on Transportation Electrification*, vol. 5, no. 1, pp. 262–270, 2019.

[32] J. Liang, P. D. Walker, J. Ruan, H. Yang, J. Wu, and N. Zhang, "Gearshift and brake distribution control for regenerative braking in electric vehicles with dual clutch transmission," *Mechanism and Machine Theory*, vol. 133, pp. 1–22, 2019.